Low-altitude electron acceleration due to multiple flow-bursts in the magnetotail

ARTICLE · FEBRUARY 2014

DOI: 10.1002/2013GL058982

AGU PUBLICATIONS

Geophysical Research Letters

RESEARCH LETTER

10.1002/2013GL058982

Key Points:
- First observation of multiple flow signatures on near-conjugate flux tubes
- Low-energy electron profile suggests Alfvénic acceleration due to fast flow
- Multiple flow bursts are obtained to extend over large radial distance in tail

Supporting Information:
- Readme
- Figure S1
- Figure S2

Correspondence to:
R. Nakamura,
rumi.nakamura@oeaw.ac.at

Citation:
Nakamura, R., T. Karlsson, M. Hamrin, H. Nilsson, O. Marghitu, O. Amm, C. Bunescu, V. Constantinescu, H. U. Frey, A. Keiling, J. Semeter, E. Sorbalo, J. Vogt, C. Forsyth, and M. V. Kubyshkina (2014), Low-altitude electron acceleration due to multiple flow bursts in the magnetotail, *Geophys. Res. Lett.*, *41*, 777–784, doi:10.1002/2013GL058982.

Received 7 DEC 2013
Accepted 10 JAN 2014
Accepted article online 13 JAN 2014
Published online 15 FEB 2014

Low-altitude electron acceleration due to multiple flow bursts in the magnetotail

R. Nakamura[1], T. Karlsson[2], M. Hamrin[3], H. Nilsson[4], O. Marghitu[5], O. Amm[6], C. Bunescu[5], V. Constantinescu[5], H. U. Frey[7], A. Keiling[7], J. Semeter[8], E. Sorbalo[9], J. Vogt[9], C. Forsyth[10], and M. V. Kubyshkina[11]

[1]Space Research Institute, Austrian Academy of Sciences, Graz, Austria, [2]Space and Plasma Physics, Royal Institute of Technology, Stockholm, Sweden, [3]Department of Physics, Umeå University, Umeå, Sweden, [4]Swedish Institute of Space Physics, Kiruna, Sweden, [5]Institute for Space Sciences, Bucharest, Romania, [6]Finnish Meteorological Institute, Helsinki, Finland, [7]Space Sciences, Laboratory, University of California, Berkeley, California, USA, [8]Department of Electrical and Computer Engineering, Boston University, Boston, Massachusetts, USA, [9]School of Engineering and Science, Jacobs University Bremen, Bremen, Germany, [10]UCL Mullard Space Science Laboratory, Dorking, UK, [11]Earth Physics Department, St. Petersburg State University, St. Petersburg, Russia

Abstract At 10:00 UT on 25 February 2008, Cluster 1 spacecraft crossed the near-midnight auroral zone, at about 2 R_E altitude, while two of the Time History of Events and Macroscale Interactions During Substorms (THEMIS) spacecraft, THD and THE, observed multiple flow bursts on the near-conjugate plasma sheet field lines. The flow shear pattern at THEMIS was consistent with the vortical motion at duskside of a localized flow channel. Coinciding in time with the flow bursts, Cluster 1 observed bursts of counterstreaming electrons with mostly low energies (≤441 eV), accompanied by short time scale (<5 s) magnetic field disturbances embedded in flow-associated field-aligned current systems. This conjugate event not only confirms the idea that the plasma sheet flows are the driver of the kinetic Alfvén waves accelerating the low-energy electrons but is a unique observation of disturbances in the high-altitude auroral region relevant to the multiple plasma sheet flows.

1. Introduction

Localized high-speed jets, called bursty bulk flows (BBF), have been known to contribute a major part of the Earthward magnetic flux and energy transport in the magnetotail [e.g., *Baumjohann et al.*, 1989]. Flow and magnetic shear observations around a BBF [e.g., *Sergeev et al.*, 1996] as well as conjugate auroral signatures [e.g., *Nakamura et al.*, 2001; *Sergeev et al.*, 2004] suggest the formation of a field-aligned current (FAC) system that consists of upward (downward) currents at the duskside (dawnside) of the localized flows. This supports the idea that the fast plasma flow is a flux tube with enhanced magnetic field and reduced plasma content, compared to the surrounding plasma, convecting Earthward due to the localized polarization electric field in the dawn-dusk direction, known as the plasma bubble model [e.g., *Chen and Wolf*, 1999]. The localized twin-cell vortex pattern and FAC associated with BBFs have been confirmed by recent multipoint observations [e.g., *Forsyth et al.*, 2008; *Keiling et al.*, 2009].

Multiple BBFs have been identified in many studies including the earlier studies of BBFs [e.g., *Sergeev et al.*, 1996], which suggest multiple sources of BBFs in time and space. More recently, it has been suggested that the enhanced pressure gradient in the near-Earth region causes the Earthward flows to bounce back not only once but for several cycles, to be observed as multiple flow enhancements [*Panov et al.*, 2010]. A damped oscillatory motion due to overshoots of the Earthward moving plasma bubble from its equilibrium position has been predicted in the MHD bubble models [*Chen and Wolf*, 1999; *Wolf et al.*, 2012] with a frequency comparable to the observed flow oscillation [*Panov et al.*, 2013].

In addition to these MHD-scale flow and field disturbances of the BBF plasma and its surroundings, low-frequency electromagnetic fluctuations on kinetic scales have been identified to be embedded within fast flows. Based on comparison of Poynting flux between $X_{GSE} = -18\ R_E$ and $-5\ R_E$, *Angelopoulos et al.* [2002] suggested that kinetic Alfvén waves radiated from BBFs in the tail are connected to large Alfvénic Poynting fluxes, as observed above the auroral oval [e.g., *Wygant et al.*, 2000]. *Chaston et al.* [2012] statistically showed that the kinetic Alfvén waves, which can contribute on average ~5% of the total energy transport, are

continuously radiated outward from the flows. Auroral electrons accelerated by small-scale Alfvén waves, e.g., fields varying on the time scale of seconds, within comparable time to the electron transit time through the auroral acceleration region, have been reported at low altitudes ($< 1\ R_E$) by *Chaston et al.* [2003]. While these electrons observed by *Chaston et al.* [2003] were often downgoing, or at times counterstreaming, Cluster observations near perigee (about 2–3 R_E) indicated that the accelerated electrons by the Alfvén waves were either upgoing or counterstreaming [*Hull et al.*, 2010; *Marklund et al.*, 2011]. These observations are consistent with the estimate that most of the Alfvénic auroral acceleration responsible for the low-energy electrons (up to about 1 keV) takes place at 1–2 R_E on the nightside [*Chaston et al.*, 2003].

In spite of this general understanding of BBFs and their coupling to the ionosphere via FACs, auroral precipitation, and Alfvén waves, there have been very few spacecraft observations providing information along the flux tubes that can link the ionosphere and auroral acceleration region to the BBFs in the magnetosphere, possibly because of the dynamic and localized signatures of the BBFs. In this study, we report observations when Cluster was at about 2 R_E altitude mostly above the auroral acceleration region but at much lower altitude compared to the near-conjugate Time History of Events and Macroscale Interactions During Substorms (THEMIS) spacecraft THD and THE, which detected three successive flow enhancements in the plasma sheet.

2. Cluster and THEMIS Near-Conjugate Observations

On 25 February 2008, between 10:00 and 10:30 UT, the four Cluster spacecraft successively crossed the high (about 2 R_E) altitude near-midnight auroral region at a close local time to the THEMIS THD and THE spacecraft during two localized activations seen in the ground magnetograms with a maximum AE ~350 nT. (The equivalent current distribution at 10:05:30 UT is shown in Figure S1 in the supporting information.) The THEMIS spacecraft observed successive dipolarizations (enhancements in B_Z) in the plasma sheet starting at 10:02.9 UT and 10:28.7 UT (Figures 1a and 1b). Cluster 1 (C1) reached the nearest point to the THE and THD foot points at 10:00 UT, C2 at 10:15 UT, and C3,C4 at 10:17 UT (dashed lines in Figures 1a and 1b).

The magnetic field configuration calculated using the adapted time-dependent magnetospheric model [*Kubyshkina et al.*, 2009] is shown in Figures 1c–1e in which the field lines crossing the different spacecraft are shown. The standard Tsyganenko model (T96) was modified to match the magnetic field observed by Cluster, THEMIS, and Geotail spacecraft, as shown in the figure. Cluster spacecraft were located at about 2 R_E altitude above the northern auroral oval near midnight local time. THE and THD were located at the same local time sector at the premidnight side as shown in Figure 1e. A drastic change from a taillike configuration (10:03 UT) to dipolar configuration (10:04 UT) can be seen in the model field, which is due to the localized dipolarization observed at midnight spacecraft. Consequently, Cluster, THD, and THE were engulfed in a more dipolar field at 10:04 UT on closed flux tubes with equatorial distances between 12 and 25 R_E. In this paper we discuss the relationships between the particle signatures observed by C1 and disturbances detected at THD and THE in the near-conjugate magnetosphere region during the dipolarization event starting at 10:02.9 UT.

C1 went out from the plasma sheet toward the polar cap at 10:02.3 UT for about 1 min, as can be seen by the dropout of the high-energy ions (> 6 keV) (Figure 2a) and keV electrons (Figure 2b). (The white areas at 10:00.5 UT in Figure 2a and at 10:00.0–10:00.1 UT in Figure 2b are data gaps.) The high-energy ions as well as keV electrons reappear between 10:03.2 UT and 10:09.1, indicating plasma sheet recovery. Note that the start of this reentry into the plasma sheet region coincides well with the start of the dipolarization shown by the increase of the magnetic field inclination angle to equatorial plane, θ, (Figure 2g) accompanied by the start of enhanced magnetic activity on the ground near the foot point of the spacecraft (Figures 2h and S1).

During the plasma sheet reentry, the ions show several enhancements at high energies, with loss-cone distribution, as well as continuous features of low-energy (< 5 keV) ion conics (Figure 2a and Figure S2 in the supporting information for details). Note that there are three episodes of enhancements in the low-energy electrons ($\leq$441 eV) during the plasma sheet reentry interval (Figure 2b) as can be identified in the differential energy flux integrated over all pitch angels and over energies 44 eV to 441 eV, shown in Figure 2c (black curve). The enhancements started at 10:03.5, 10:05.5, and 10:08.1 UT (indicated by vertical dashed lines) with times of maximum energy flux at 10:04.7, 10:06.2, and 10:08.7 UT. The electrons therefore consist of two components: the rather continuous hot plasma sheet component and the low-energy electron bursts. The pitch angle distribution of electrons between 44 eV and 441 eV (Figure 2j) and the selected distribution functions (Figure 2k) show that the counterstreaming low-energy electrons are often dominated by upward

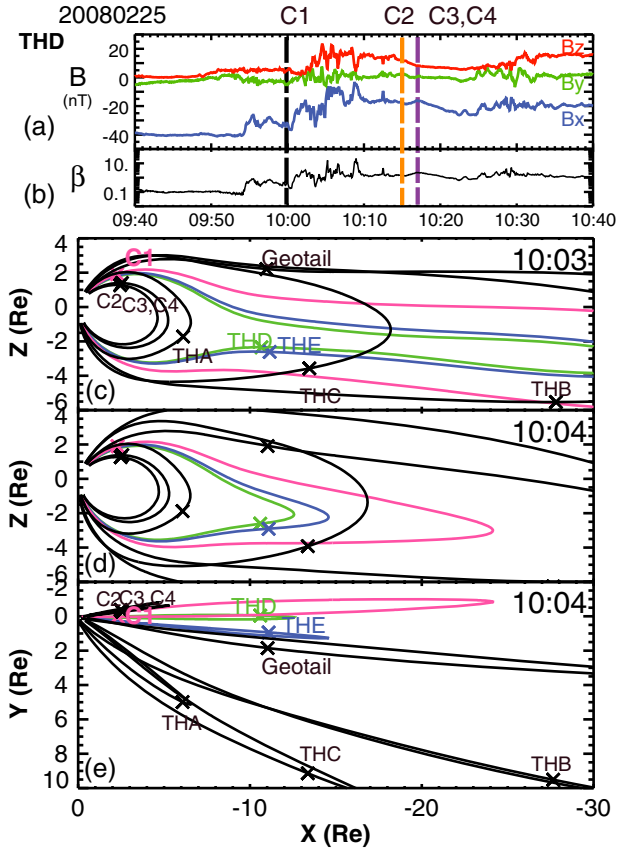

Figure 1. (a) Magnetic field and (b) ion beta from the THEMIS spacecraft THD between 09:40 and 10:40 UT. The times when the four Cluster spacecraft were nearest conjugate to THD and THE are indicated with dashed lines. Magnetic field lines calculated using the adapted time-dependent magnetospheric model [*Kubyshkina et al.*, 2009] crossing the different spacecraft at (c) 10:03 UT and at (d) 10:04 UT projected in the *X-Z* plane and at (e) 10:04 UT projected in the *X-Y* plane.

(180°) electrons up to about 1–2 keV but sometimes extending to higher energy (10:04:42 UT panel). At Cluster altitude, such counterstreaming electrons have earlier been interpreted as Alfvénic accelerated electrons [*Hull et al.*, 2010; *Marklund et al.*, 2011].

The dipolarization was associated with bursts of high-speed flows observed at THD and THE as can be seen in the profiles of the ion flow speeds perpendicular to the magnetic field (Figure 2c, blue and purple curves). Three episodes of enhanced flows were observed by both THD and THE. The enhanced flows at THD started at 10:02.9, 10:05.3, and 10:08.2 UT and with maximum total flow speed of 856 km/s at 10:04.5 UT, 557 km/s at 10:06.4 UT, and 323 km/s at 10:08.4 UT. The flows at THE started at 10:03.0, 10:04.8, and 10:08.0 UT, with maximum speed of 543 km/s at 10:04.2 UT, 448 km/s at 10:06.0 UT, and 252 km/s at 10:09.0 UT. These three pulses of enhanced flows therefore coincide well with the periods of enhanced low-energy electrons at C1 (Figure 2c). For example, the peak times of the flow at THD and those of the electron flux at C1 agree within 20 s differences. These observations therefore suggest that there is a good correlation between the fast flow in the tail and Alfvénic acceleration of electrons at low altitude. A better coincidence of THD is expected due to closer distance between the foot points of THD and C1 compared to THE and C1. For convenience, in the following we call these three enhancements the 10:04 UT, 10:06 UT, and 10:08 UT events.

The signals detected by C1 are expected to be delayed compared to the THD/THE measurements, due to the propagation time along the field line. The Alfvén travel time between C1 and THD/THE is estimated based on the *X* location of the spacecraft and using average values of the model field lines crossing THE, THD, and C1 (Figure 1) by assuming north-south symmetry and a density of 0.5/cc. The estimated times are 23 s (10:03 UT), 24 s (10:04 UT), 26 s (10:06 UT), and 25 s (10:08 UT), which are comparable to the time differences between electron flux enhancements C1 and flow bursts at THD or THE. Assuming that the main driver producing the enhanced field-aligned electron profiles are kinetic Alfvén waves, this timing can be considered

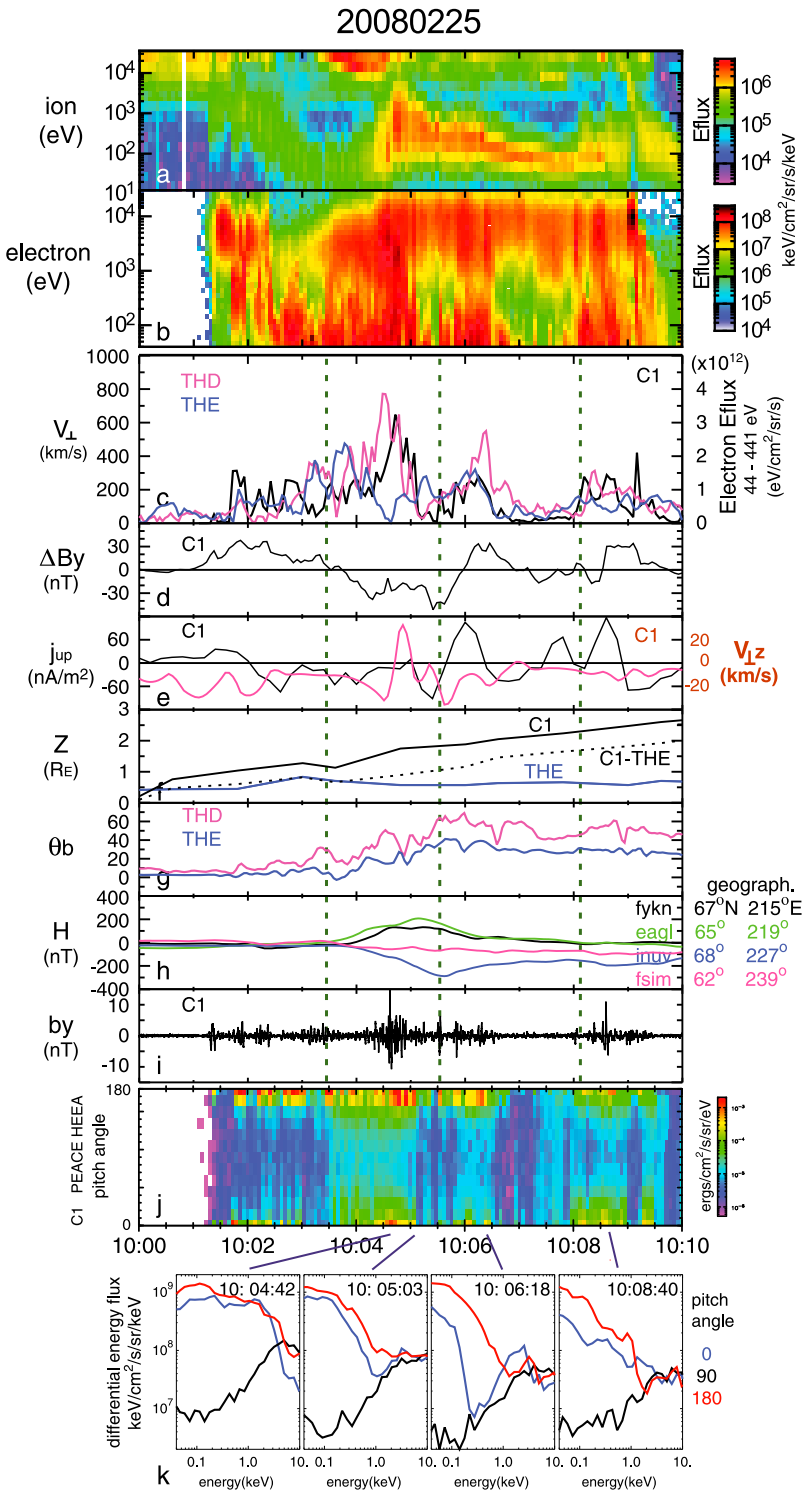

Figure 2. C1, THD, THE, and ground-based observations: (a) ion and (b) electron energy spectra from C1; (c) low-energy (44–441 eV) electron energy flux from C1 and plasma flow speed perpendicular to the magnetic field observed by THD and THE; (d) dawn-to-dusk magnetic field disturbance and (e) upward field-aligned current (black line) and northward flow component perpendicular to the magnetic field (red) from C1; (f) the Z location of the field lines passing C1 (black line) and THE (blue line) and the difference between the two (dotted line) at $X = -8\ R_E$; (g) the latitude angle of the magnetic field from THD and THE; (h) H component from the ground stations near the THD foot point; (i) magnetic field disturbance (0.2–10 Hz); (j) low-energy electron pitch angle spectrograms; and (k) parallel, perpendicular, and antiparallel electron distributions for selected times from C1. Vertical lines indicate the start of the enhanced low-energy electron flux interval, 10:03.5, 10:05.5, and 10:08.1 UT.

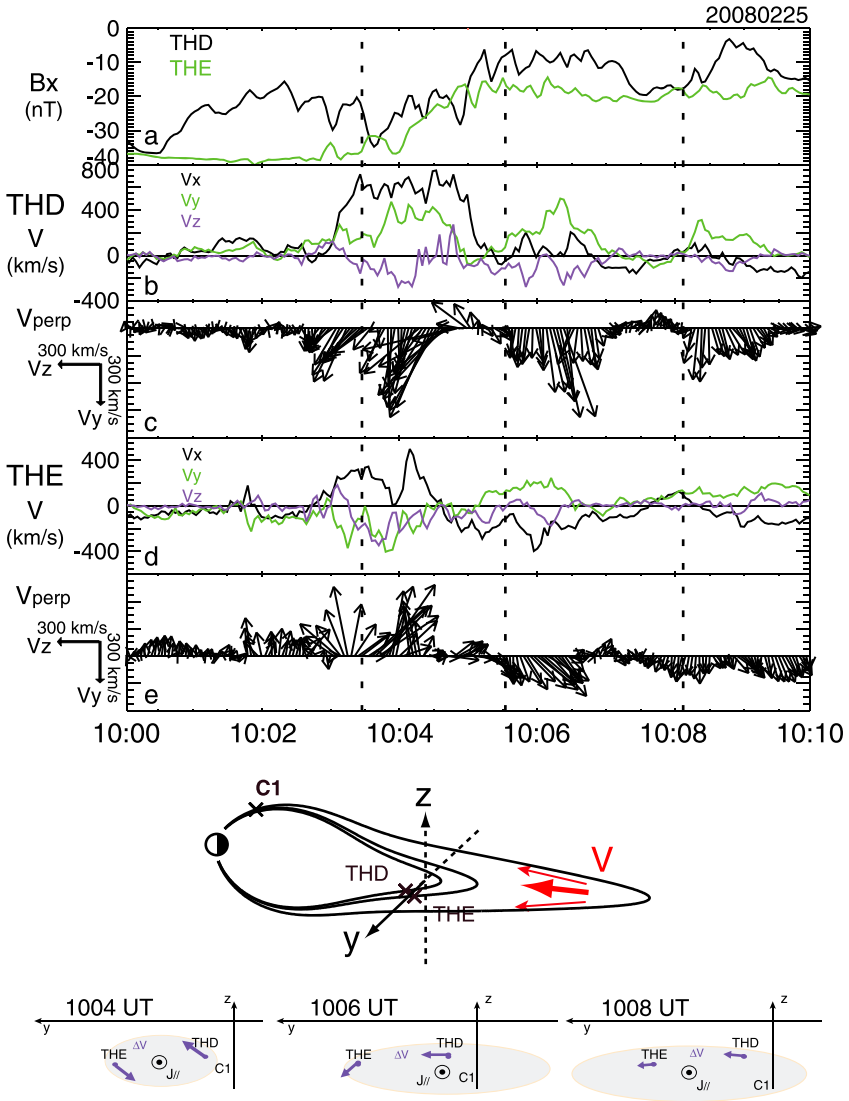

Figure 3. (a) The B_X component from THD and THE, (b) the three components of the ion flow, and (c) perpendicular flow vectors in the *Y-Z* plane from THD. (d,e) Same as Figures 3b and 3c but for THE. The vertical lines show the same start times of the low-energy electron events shown in Figure 2. (bottom) The relationships between the THD/THE vortex and the possible C1 location related to this structure during the three flow burst events is sketched around the maximum time of the THEMIS flow bursts, 10:04, 10:06, and 10:08 UT.

as the maximum shift in the coupling times. Hence, the overall good relationship between C1 and THD/THE observations is preserved even when taking into account the Alfvén transit time.

Cluster went out into the polar cap region at 10:09.1 UT. This plasma sheet exit at 10:09.1 UT as well as the one before at 10:02.3 UT is followed by enhancements in the low-energy electrons which can be interpreted as Alfvénic accelerated electrons. These low-energy electron features may therefore be a more persistent structure near the polar cap boundary. Indeed, similar features of low-energy electrons near the polar cap boundary were also detected by the other Cluster spacecraft, while the plasma sheet reentry event was not observed by these spacecraft (not shown). These differences support the idea that the striking temporal correlation between the magnetospheric flows and the low-energy electron flux increases are due to temporal changes in the magnetosphere.

Figure 2d shows the azimuthal (near dawn-to-dusk) magnetic field component, $\triangle B_Y$, from C1 in the mean field-aligned coordinates, which is an indicator of a FAC. The dawn-to-dusk direction is defined as $\mathbf{R} \times \mathbf{B_0}$, where $\mathbf{R}$ is the spacecraft position vector and $\mathbf{B_0}$ is the 8 min average of the magnetic field. Assuming a spacecraft motion mainly northward relative to a planar FAC sheet, a positive (negative) slope corresponds

to an upward (downward) FAC. Such an assumption would be valid before the dipolarization, i.e., between 10:00 and 10:03 UT and well after 10:06 UT. It is not the case, however, during the expansion of the plasma sheet, which suggests a change toward a dipolar configuration. This change of the field configuration can also be seen in the temporal profile of the Z location of the field lines passing C1 and THE at $X = -8\ R_E$ shown in Figure 2f. The increasing trend in Z position for C1 shows the poleward motion of the spacecraft. Around 10:03 UT, however, Z position slightly decreases, reflecting the change to dipolar configuration. As a consequence, the FAC may have crossed the spacecraft in an opposite direction (northward) during the plasma sheet expansion, which means that the spacecraft detects the FAC from poleward side to equatorward side. Furthermore, the FAC sheet may well propagate Earthward (or equatorward at this location) associated with the Earthward flow burst in the tail. Indeed, such a motion can be seen in the vertical (Z) component of the plasma flow perpendicular to the magnetic field (red trace in Figure 2e). That is, enhancements of equatorward (negative V_Z) flow were detected during the flow bursts except for 10:04 UT event (first dashed line) when the initial negative V_Z was followed by enhanced poleward plasma motion, as is expected due to the change in the current sheet toward a more dipolar configuration. Since a definite motion of FAC cannot be obtained from a single spacecraft, we use the plasma and the spacecraft motion (the former being up to 10 times faster than the latter) to estimate the FAC density (Figure 2e, positive for upward current). Due to the above uncertainties in the crossing direction of the FAC during the plasma sheet expansion, we have not estimated the FAC between 10:03.8 and 10:05.5 UT. Enhancements in upward FAC followed by downward FAC current were seen for 10:06 and 10:08 UT events (Figure 2e) which corresponds to the positive and negative slopes in B_Y disturbance (Figure 2d). Due to the general poleward motion of the spacecraft and due to the expected FAC motion associated with the plasma motion, the spacecraft crossed the FAC from equatorward side to poleward side for these two events. Hence, the overall current system of increased electron flux intervals consists of mainly upward FAC on the low-latitude side with weaker downward current on the high-latitude side. Such patterns are consistent with the duskside part of the FAC system obtained for localized flow bursts in the magnetotail [*Birn et al.*, 2004, Figure 17].

During these flow-associated FAC enhancements, enhanced small-scale magnetic field fluctuations are observed as shown in Figure 2i. The same dawn-dusk component of the magnetic field, b_Y, as in Figure 2d, but bandpass-filtered (0.2–10 Hz) high-resolution (22.4 Hz) data are shown. While these magnetic fluctuations only suggest a possibility of existence of Alfvén wave activity, it is interesting to note that the enhancements in these fluctuations were accompanied by the enhancement of the field-aligned low-energy electrons (Figure 2j). For the observed typical plasma motion of 5–20 km/s with respect to spacecraft and the ion temperatures range of 1–10 keV, the fluctuations will have comparable scale to $2\pi\rho_i$, where ρ_i is the ion gyroradius, when this is less than 10–32 km or for time scale less than 0.5–6 s. In this case, the kinetic effect may play a role. Although the C1 location does not necessarily correspond to the acceleration site of these electrons, Figure 2i confirms that the embedded short time scale (<5 s) wave effects may be expected in the flow burst disturbed flux tubes.

At THEMIS the Earthward component was the largest component in the total flow (Figures 3b and 3d), and higher speed of the flows were observed at THD, which is likely to be closer to the central local time of the flows as well as closer to the current sheet center as can be seen by the lower B_X magnitude (Figure 3a). The flow shear patterns at THD and THE are examined based on the flow vectors perpendicular to the magnetic field in the Y-Z plane. We chose this plane because of the relatively low field inclination angle (Figure 2g) of the two THEMIS spacecraft that are separated mainly along the dawn-dusk direction, such that the perpendicular flow direction was observed mainly in this plane. The 10:04 UT event is associated with duskward-northward perpendicular flow for THD (Figure 3c) and dawnward-southward perpendicular flow for THE (Figure 3e), suggesting that they are located at both sides of the anticlockwise vortex viewed from the tail (see Figure 3 (bottom) 10:04 UT panel). The 10:06 UT event is associated with duskward and slightly northward then turning to duskward-southward perpendicular flow for THD, while duskward-southward perpendicular flow was detected at THE, indicating a larger vortex centered southward of both spacecraft as illustrated in 10:06 UT panel in Figure 3 (bottom). Both THD and THE observed again duskward but weak flow for the 10:08 UT event, suggesting an extended vortex region south of the spacecraft. All these flows therefore create a vortex pattern which is expected at the duskside of the flow burst, where the flow-associated FAC direction is expected to be conjugate to an upward current region. Assuming north-south symmetry for the current sheet evolution, a conjugate location of flux tube crossing of C1 in the Southern Hemisphere in the Y-Z plane would be south of THE and on the midnight side of THD as

indicated in Figure 3 (bottom). For the 10:04 UT event, C1 was likely located at the dawnside edge of the flow vortex, which was close to the center of the flow burst. This might be another reason for the absence of FAC at C1 in Figure 2 for the 10:04 UT event. The predominant upward FAC for C1 during the 10:06 UT and 10:08 UT events (Figure 2) is consistent with the location of the more elongated and southward shifted vortex observed in the tail.

3. Discussion and Conclusions

Hull et al. [2010] obtained the temporal evolution of a density cavity using data from consecutive crossings of the high-altitude auroral region by multipoint Cluster. For the event discussed in this paper, the crossing took place during activations in the magnetosphere so that temporal changes are identified within the C1 crossing period based on comparison with magnetospheric observations. This conjugate event not only confirms the idea that the plasma sheet flows drive kinetic Alfvén waves accelerating the low-energy electrons but also presents a unique observation of disturbances at about 2 R_E altitude above the auroral oval, relevant to the multiple plasma sheet flows.

The THEMIS flow shear observations suggest that the flow vortex at the later times is centered farther away from THEMIS, i.e., away from the equator, which can be interpreted as due to the BBF-associated local expansion of the plasma sheet. This is consistent with results from the field modeling near midnight, which show that the equatorial crossing point of the THD field lines changes from $X = -34.4\ R_E$ to $-11.6\ R_E$ during the three flow events. Note, however, that during these three flow bursts, Cluster 1 moved poleward, covering further tailward field lines. The motion can be seen in the increasing Z location in Figure 2f. The equatorial distances of these field lines are 24.3 R_E (10:04 UT) and 57.9 R_E (10:08 UT) in the model. The relative motion of Cluster and THD/THE spacecraft suggests that these multiple flow bursts are extended in radial direction, possibly along the flow channel, including the later events. This is somewhat unexpected in a damped flux-tube oscillation scenario where the later flow pulses involve only the near-Earth region. Hence, these three flow events are difficult to interpret as a damped oscillation of flux tubes around one equilibrium distance in the near-Earth flow-braking region, although some reversals of Earthward to tailward flows are seen in Figure 3. Tailward retreat in the equilibrium distance due to magnetic flux pileup for later flow burst events may need to be taken into account. Alternatively, there can be three flow pulses from three activations with bouncing and immediate damping.

Although the major contributing force in the flow-braking process would be the force imbalance in the magnetosphere [e.g., *Birn et al.*, 2004], the ionosphere certainly is expected to play an important role in the evolution of the flows since the entire flow braking takes longer than the bouncing of the Alfvén waves. Further quantitative investigations using ionospheric parameters are planned for future studies.

Acknowledgments

This work is based on a collaborative effort of the ISSI Team 200 led by O. Marghitu and J. Vogt and the FP7 European Cluster Assimilation Technology (ECLAT) team. The authors acknowledge the support of the International Space Science Institute (ISSI), Bern. We acknowledge I. Dandouras, A. Fazakerley, C. Carr, and CAA team for the use of Cluster data and NASA contract NAS5-02099 and V. Angelopoulos, C.W. Carlson, J.P. McFadden, D. Larson, R.P. Lin, K.H. Glassmeier, U. Auster, and W. Baumjohann for the use of THEMIS data, T. Nagai for Geotail data, C.T. Russell, S. Mende, and Geophys. Inst./Univ. Alaska for GMAG data, and J.M. Weygand for SECS analysis. The work was supported by the Austrian Science Fund FWF I429-N16 and P23862-N16, NSF grant AGS-1004736, NASA grants NNX12AK38G and NAS5-02099, M-ICAR grant of the Romanian National Authority for Scientific Research PN-II-ID-PCE-2011-3-1013, and the ALEOS contract 20/2012 with Romanian Space Agency. C.F. was funded by STFC consolidated grant ST/K000977/1.

The Editor thanks two anonymous reviewers for their assistance in evaluating this paper.

References

Angelopoulos, V., J. A. Chapman, F. S. Mozer, J. D. Scudder, C. T. Russell, K. Tsuruda, T. Mukai, T. J. Hughes, and K. Yumoto (2002), Plasma sheet electromagnetic power generation and its dissipation along auroral field lines, *J. Geophys. Res.*, *107*(A8), SMP 14-1–SMP 14-20, doi:10.1029/2001JA900136.

Baumjohann, W., G. Paschmann, N. Scopke, and C. A. Cattell (1989), Average plasma properties in the central plasma sheet, *J. Geophys. Res.*, *94*, 6597–6606.

Birn, J., J. Raeder, Y. L. Wang, R. A. Wolf, and M. Hesse (2004), On the propagation of bubbles in the geomagnetic tail, *Ann. Geophys.*, *22*, 1773–1786.

Chaston, C. C., J. W. Bonnell, C. W. Carlson, J. P. McFadden, R. E. Ergun, and R. J. Strangeway (2003), Properties of small-scale Alfveén waves and accelerated electrons from FAST, *J. Geophys. Res.*, *108*, 8003, doi:10.1029/2002JA009420.

Chaston, C. C., J. W. Bonnell, L. Clausen, and V. Angelopoulos (2012), Energy transport by kinetic-scale electromagnetic waves in fast plasma sheet flows, *J. Geophys. Res.*, *117*, A09202, doi:10.1029/2012JA017863.

Chen, C. X., and R. A. Wolf (1999), Theory of thin filament motion in Earth's magnetotail and its application to bursty bulk flows, *J. Geophys. Res.*, *104*, 14,613–14,626, doi:10.1029/1999JA900005.

Forsyth, C., et al. (2008), Observed tail current systems associated with bursty bulk flows and auroral streamers during a period of multiple substorms, *Ann. Geophys.*, *26*, 167–184, doi:10.5194/angeo-26-167-2008.

Hull, A. J., M. Wilber, C. C. Chaston, J. W. Bonnell, J. P. McFadden, F. S. Mozer, M. Fillingim, and M. L. Goldstein (2010), Time development of field-aligned currents, potential drops, and plasma associated with an auroral poleward boundary intensification, *J. Geophys. Res.*, *115*, A06211, doi:10.1029/2009JA014651.

Keiling, A., et al. (2009), Substorm current wedge driven by plasma flow vortices: THEMIS observations, *J. Geophys. Res.*, *114*(13), A00C22, doi:10.1029/2009JA014114.

Kubyshkina, M., V. Sergeev, N. Tsyganenko, V. Angelopoulos, A. Runov, H. Singer, K. H. Glassmeier, H. U. Auster, and W. Baumjohann (2009), Toward adapted time-dependent magnetospheric models: A simple approach based on tuning the standard model, *J. Geophys. Res.*, *114*, A00C21, doi:10.1029/2008JA013547.

Marklund, G. T., S. Sadeghi, T. Karlsson, P.-A. Lindqvist, H. Nilsson, C. Forsyth, A. Fazakerley, E. A. Lucek, and J. Pickett (2011), Altitude distribution of the auroral acceleration potential determined from Cluster satellite data at different heights, *Phys. Rev. Lett.*, *106*, 055,002, doi:10.1103/PhysRevLett.106.055002.

Nakamura, R., W. Baumjohann, M. Brittnacher, V. A. Sergeev, M. Kubyshkina, T. Mukai, and K. Liou (2001), Flow bursts and auroral activations: Onset timing and foot point location, *J. Geophys. Res.*, *106*, 10,777–10,789.

Panov, E., et al. (2010), Multiple overshoot and rebound of a bursty bulk flow, *Geophys. Res. Lett.*, *37*, L08103, doi:10.1029/2009GL041971.

Panov, E. V., M. V. Kubyshkina, R. Nakamura, W. Baumjohann, V. Angelopoulos, V. A. Sergeev, and A. A. Petrukovich (2013), Oscillatory flow braking in the magnetotail: THEMIS statistics, *Geophys. Res. Lett.*, *40*, 2505–2510, doi:10.1002/grl.50407.

Sergeev, V., V. Angelopulous, J. T. Gosling, C. A. Cattell, and C. T. Russell (1996), Detection of localized, plasma-depleted flux tubes or bubbles in the midtail plasma sheet, *J. Geophys. Res.*, *101*, 10,817–10,826.

Sergeev, V., K. Liou, P. Newell, S. Ohtani, M. Hairston, and F. Rich (2004), Auroral streamers: Characteristics of associated precipitation, convection and field-aligned currents, *Ann. Geophys.*, *22*, 537–548, doi:10.5194/angeo-22-537-2004.

Wolf, R. A., C. X. Chen, and F. R. Toffoletto (2012), Thin filament simulations for Earth's plasma sheet: Interchange oscillations, *J. Geophys. Res.*, *117*(16), A02215, doi:10.1029/2011JA016971.

Wygant, J. R., et al. (2000), Polar spacecraft based comparisons of intense electric fields and Poynting flux near and within the plasma sheet-tail lobe boundary to UVI images: An energy source for the aurora, *J. Geophys. Res.*, *105*, 18,675–18,692, doi:10.1029/1999JA900500.